SUPPLEMENTAL MATERIAL

Ecto-5'-nucleotidase (CD73) inhibits nociception by hydrolyzing AMP to adenosine in nociceptive circuits (Sowa, Taylor-Blake, Zylka)

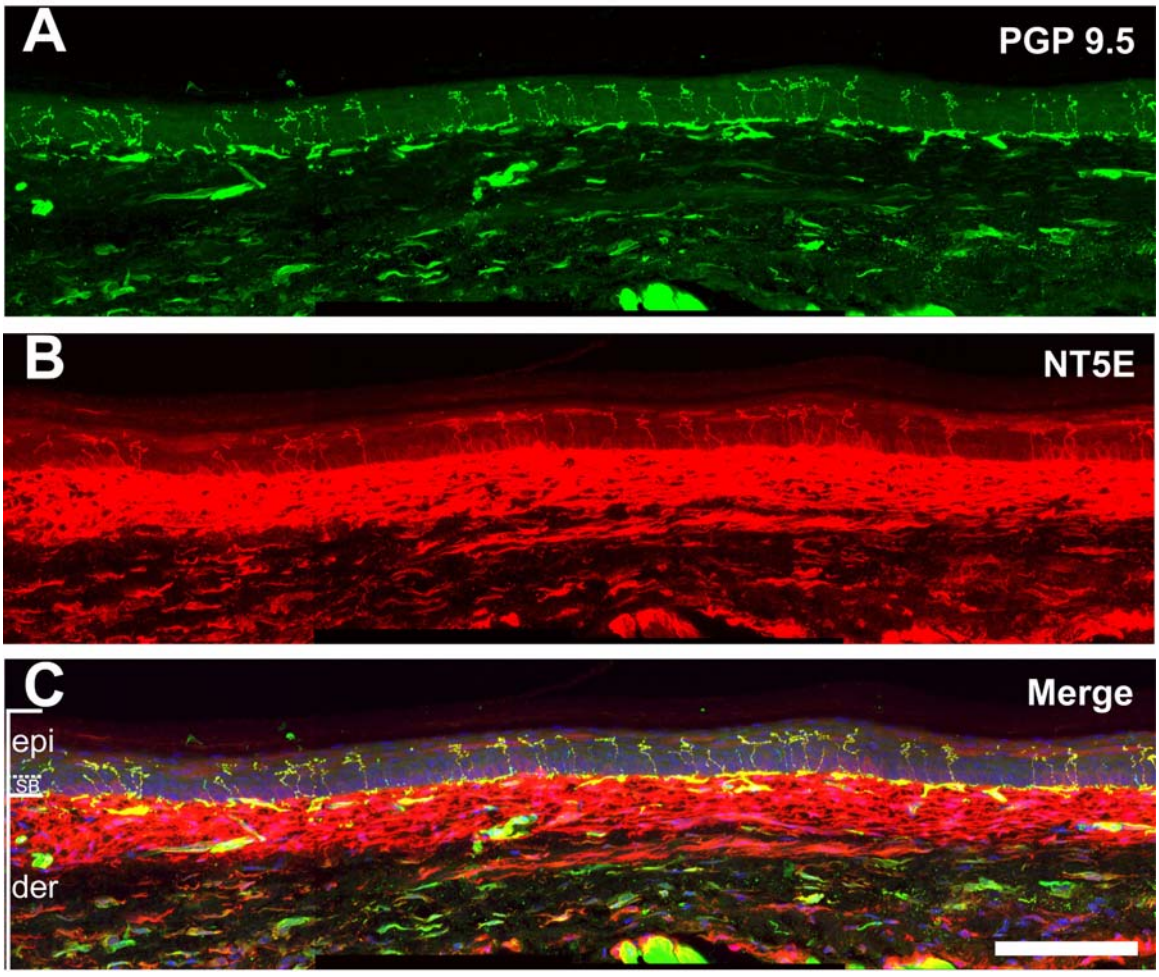

Figure S1. NT5E is localized to free nerve endings in the epidermis and to cells in the underlying dermis of glabrous skin. Photomontage encompassing the epidermis (epi) and dermis (der) of mouse glabrous skin immunostained for (A) the pan-neuronal fiber marker PGP 9.5 and (B) NT5E. NT5E was also found on keratinocytes of the stratum basalis (SB) and on cells and nerve fibers in the dermis. (C) Nuclei are pseudocolored blue to highlight stratification of the epidermis. Scale bar; 100 μm for all panels.

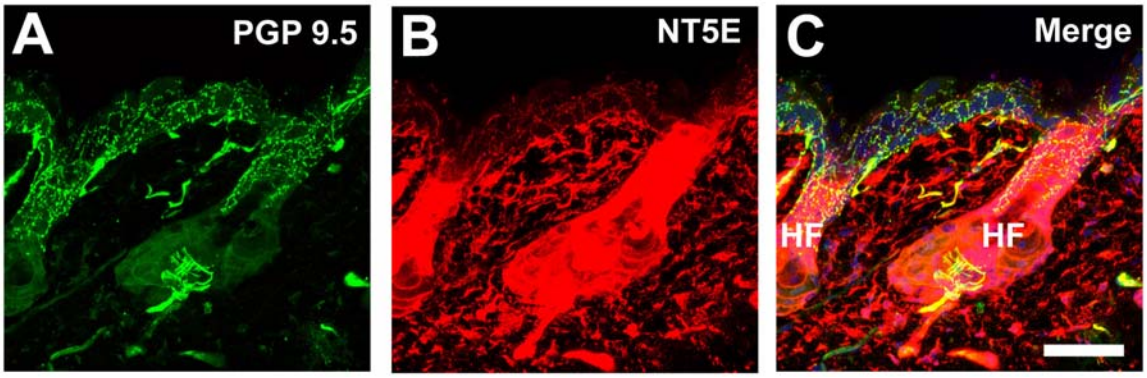

Figure S2. NT5E is localized to free nerve endings in the epidermis, to cells in the underlying dermis, and to cells that make up hair follicles (HF) in hairy skin. Confocal images of the epidermal and dermal layers of mouse hairy skin immunostained for (A) the pan-neuronal fiber marker PGP 9.5 and (B) NT5E. (C) Nuclei are pseudocolored blue to highlight stratification of the epidermis. Scale bar; 50 μm for all panels.

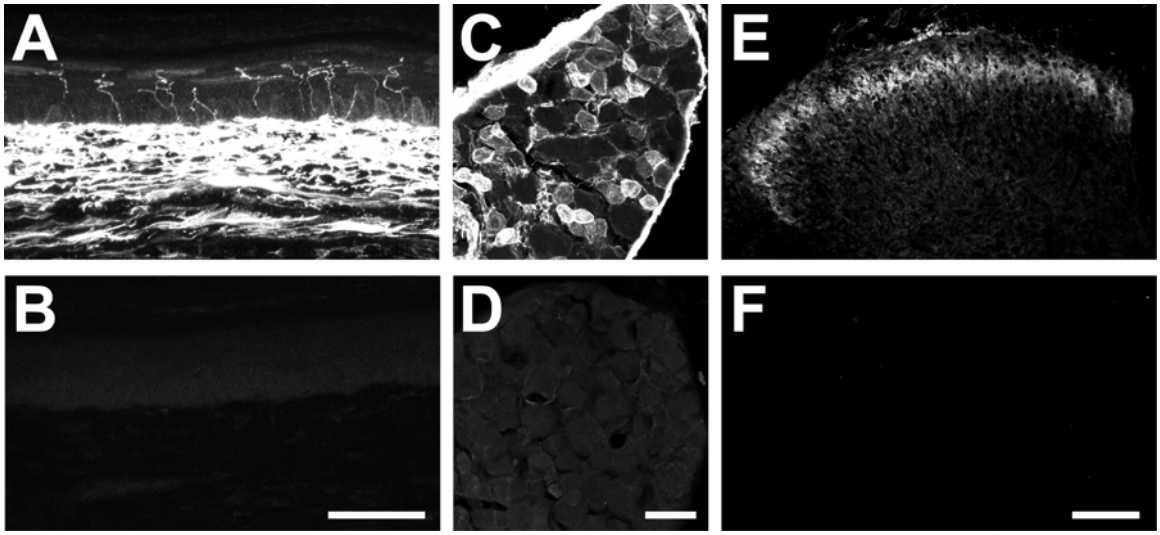

Figure S3. NT5E immunostaining of tissues from wild-type and *Nt5e*$^{-/-}$ mice. (A, B) Hindpaw glabrous skin, (C, D) lumbar DRG and (E, F) lumbar spinal cord from age-matched WT and *Nt5e*$^{-/-}$ mice were immunostained (at the same time for each image pair) using the NT5E antibody then imaged by confocal microscopy (using the same settings for each image pair). (A, C, E) WT tissues. These raw, non-pseudocolored, images reveal the complete absence of staining in tissues from *Nt5e*$^{-/-}$ mice (B, D, F). Scale bar, 50 μm for (A-D), 100 μm for (E, F).

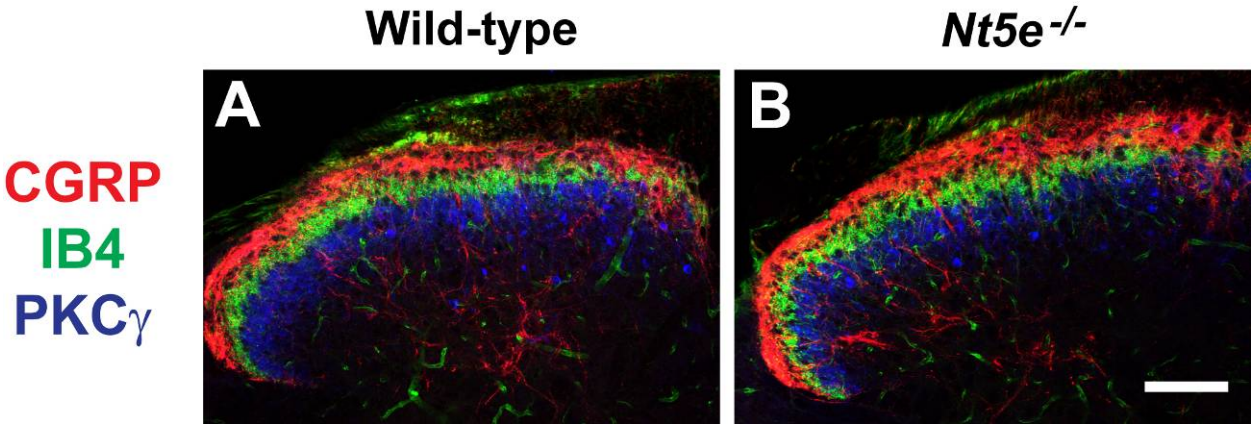

Figure S4. Axon terminals are anatomically normal in *Nt5e*$^{-/-}$ mice. Lumbar spinal cord sections from (A) wild-type and (B) *Nt5e*$^{-/-}$ mice were stained with antibodies to CGRP (to mark peptidergic nerve endings), IB4 (to mark nonpeptidergic nerve endings) and antibodies to Protein Kinase C-γ (PKCγ, to mark interneurons in laminas II_{inner} and III). Confocal image analysis revealed no gross anatomical differences between genotypes (n=2 mice from each genotype). Scale bar; 100 μm.

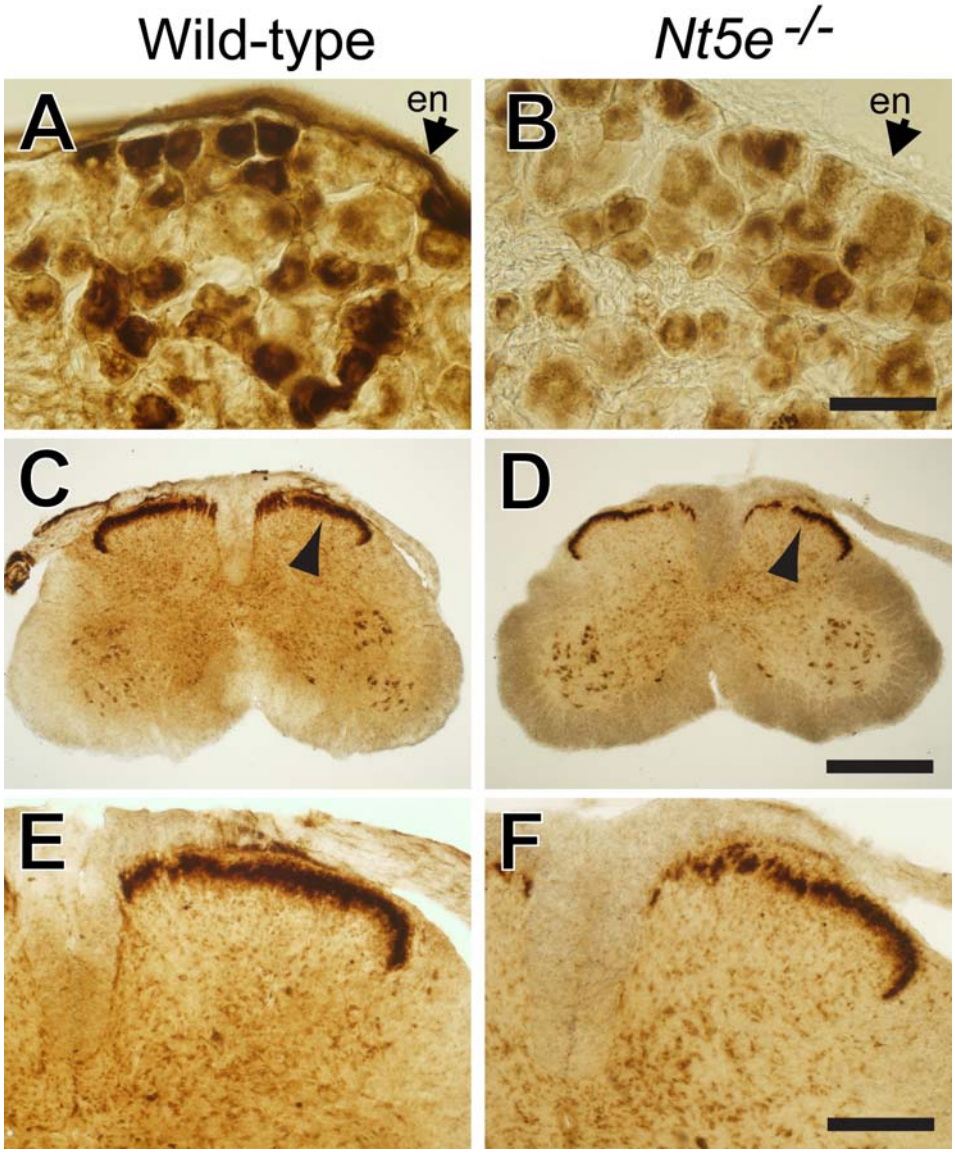

Figure S5. **AMP hydrolytic activity at acidic pH is reduced in nociceptive circuits of *Nt5e*$^{-/-}$ mice.** (A, B) Lumbar DRG and (C-F) lumbar spinal cord from wild-type and *Nt5e*$^{-/-}$ adult mice stained using AMP histochemistry. Arrows point to epineurium (en). (C, D) Arrowheads mark the location of axon terminals in dorsal spinal cord (lamina II). (E, F) Higher magnification of (C, D). AMP (1 mM in [A, B] and 3 mM in [C-F]) was used as substrate, and buffer was pH 5.6. Scale bar, 50 μm for (A, B), 500 μm for (C, D) and 200 μm for (E, F).

Table S1. Deletion of *Nt5e* does not alter the number of P2X3$^+$ or CGRP$^+$ neurons in lumbar ganglia.

	% P2X3$^+$	% CGRP$^+$
Wild-type	**45.3 ± 1.2**	**45.0 ± 1.6**
Nt5e$^{-/-}$	**44.6 ± 1.1**	**44.5 ± 0.9**
	P = 0.685	*P = 0.782*

Expressed as a percentage relative to all NeuN$^+$ neurons in L3-L5 DRG. Ganglia from three adult mice were counted per genotype. N > 5,800 NeuN$^+$ neurons were counted per marker and per genotype. Counter was blind to genotype. Data expressed as mean ± s.e.m.

Table S2. Summary of nociceptive behavioral phenotypes in *Nt5e*$^{-/-}$, *Pap*$^{-/-}$ and *A*$_1$*R*$^{-/-}$ mice relative to wild-type mice.

	Nt5e$^{-/-}$	*Pap*$^{-/-}$	*A*$_1$*R*$^{-/-}$
Hot Plate	Normal	Normal[1]	Not done
Tail Immersion / Flick	Enhanced	Normal[1,a]	Enhanced[2,3]
Thermal (Hargreaves)			
Baseline	Normal	Normal[1]	Normal[1,3]
Post inflammation	Enhanced	Enhanced[1]	Enhanced[1,3,b]
Post nerve injury	Enhanced	Enhanced[1]	Enhanced[1,3,c]
Mechanical (von Frey)			
Baseline	Normal	Normal[1]	Normal[1,3]
Post inflammation	Enhanced	Enhanced[1]	Normal[1,3,b]
Post nerve injury	Normal	Normal[1]	Normal[1,3,c]

[a] There was a nonsignificant trend towards enhanced responses in this study.
[b] Phenotype reproduced using CFA and carrageenan to inflame hindpaw.
[c] Phenotype reproduced using SNI and photochemical induction to injure peripheral nerves.
[1] Zylka, M.J. et al. (2008) Neuron 60:111-22.
[2] Johansson, B. et al. (2001) Proc Natl Acad Sci U S A 98:9407-12.
[3] Wu, W.P. et al. (2005) Pain 113:395-404.